



HAL
open science

Inverse modelling of two-dimensional water infiltration into a soil containing macropores

Adam Szymkiewicz, Jolanta Lewandowska, Rafaël Angulo-Jaramillo, Pascale Lutz

► **To cite this version:**

Adam Szymkiewicz, Jolanta Lewandowska, Rafaël Angulo-Jaramillo, Pascale Lutz. Inverse modelling of two-dimensional water infiltration into a soil containing macropores. CFM 2007 - 18ème Congrès Français de Mécanique, Aug 2007, Grenoble, France. ⟨hal-03358173⟩

HAL Id: hal-03358173

<https://hal.science/hal-03358173v1>

Submitted on 29 Sep 2021

HAL is a multi-disciplinary open access archive for the deposit and dissemination of scientific research documents, whether they are published or not. The documents may come from teaching and research institutions in France or abroad, or from public or private research centers.

L'archive ouverte pluridisciplinaire **HAL**, est destinée au dépôt et à la diffusion de documents scientifiques de niveau recherche, publiés ou non, émanant des établissements d'enseignement et de recherche français ou étrangers, des laboratoires publics ou privés.



HAL Authorization

Inverse modelling of two-dimensional water infiltration into a sand containing macropores

Adam Szymkiewicz¹, Jolanta Lewandowska², Rafael Angulo-Jaramillo^{3,4} & Pascale Lutz⁵

¹ Institute of Hydroengineering of the Polish Academy of Sciences
80328 Gdańsk, Poland, e-mail: adams@ibwpan.gda.pl

² Laboratoire Sols, Solides, Structures-Risques (3S- R)
BP 53, 38041 Grenoble, France

³ Laboratoire d'étude des Transferts en Hydrologie et Environnement (LTHE)
BP 53, 38041 Grenoble, France

⁴ Laboratoire des Sciences de l'Environnement, ENTPE
Rue Maurice Audin, 69518 Vaulx-en-Velin, France

⁵ Département Géosciences, Institut Polytechnique Lasalle Beauvais,
13 bd. de l'Hautil, 95092 Cergy cedex, France

Abstract :

Two series of axi-symmetric laboratory infiltration experiments were carried out in homogeneous sand and in sand containing artificially made vertical macropores. In the first case the results are compared with numerical solution of the Richards equation. In the second case the results are compared with the double-porosity model obtained by homogenization. The constitutive relations between the capillary pressure, saturation and unsaturated hydraulic conductivity for the sand and macropores are identified via numerical inverse analysis of cumulative infiltration. The applicability of several types of constitutive functions available in the literature is tested. The saturated conductivity and air-entry pressure fitted for the macropores are compared with theoretical predictions. The cumulative infiltration curves fitted by numerical inversion show reasonable agreement with observations for both types of porous media.

Résumé :

Deux séries d'expériences d'infiltration axy-symétrique ont été réalisées dans un sable homogène et dans le même sable contenant des macropores artificiels percés verticalement. Les données expérimentales sont comparées aux données issues de la résolution numérique de l'équation de Richards pour le cas du milieu homogène, puis pour le cas du milieu à double porosité (sable avec macropores) à partir de la méthode d'homogénéisation. Les relations caractéristiques entre la pression capillaire, l'humidité et la conductivité hydraulique pour le sable et les macropores ont été identifiées par analyse inverse de l'infiltration cumulée. Plusieurs modèles de fonctions hydrauliques provenant de la littérature ont été analysés. Les valeurs optimisées de la conductivité hydraulique et de la pression d'entrée d'air des macropores ont été ensuite comparées avec la prédiction du modèle. Les courbes d'infiltration cumulée ajustées par l'inversion numérique sont en bon accord avec les données expérimentales.

Key-words :

unsaturated flow; double-porosity; inverse analysis; macropores

1 Introduction

The presence of macropores in soil may result from various processes like shrinkage, plant growth, or soil fauna activity. These large, open pores are activated when the soil approaches full saturation (soil water pressure head close to zero), leading to accelerated infiltration and

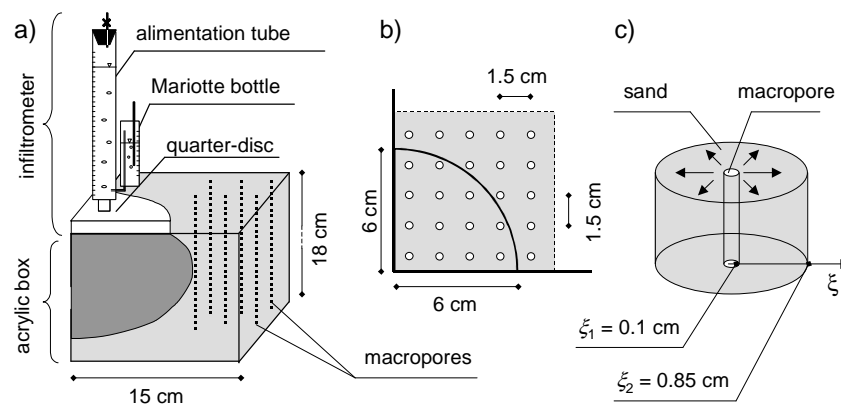


FIG. 1 – a) Experimental setup, b) Arrangement of macropores near the infiltrometer disc, c) Representation of the local-scale water transfer.

pollutant transfer. In drier conditions, water usually does not enter macropores due to their relatively large diameter and they can be treated as impermeable. The flow with active macropores can be described by a double-porosity model based on the homogenization approach, proposed by Lewandowska et al. (2004). It consists of a macroscopic scale equation for the flow in the highly conductive macropores coupled with a set of equations describing local-scale water diffusion from macropores into the sand matrix. A generalized numerical implementation of the model, suitable also for the case of inactive macropores, is presented by Szymkiewicz & Lewandowska (2006). The model requires the knowledge of the hydraulic functions (i.e. the relations between the capillary pressure, saturation and conductivity), which usually involve 2 to 6 parameters for each sub-domain. In practice the functions' parameters often have to be identified using inverse methods.

In this paper we present inverse modelling of two series of axi-symmetric infiltration experiments performed on homogenous sand and on sand with macropores, respectively (Lutz 1998). The analysis was performed in two stages. First, we used the experiments on homogeneous sand to identify the hydraulic functions of the sand by solving inverse problem for the Richards equation. Several types of hydraulic functions were examined. In the second stage we attempted to reproduce the experiments on sand with macropores using the double-porosity model (Szymkiewicz & Lewandowska 2006). The sand matrix was characterized by the previously identified parameters. The parameters of macropores were found by solving the inverse problem for the double-porosity model. They were compared with the parameters predicted theoretically on the basis of the macropore geometry.

2 Experiments

The experimental setup consisted of an acrylic box of the dimensions 15×15×18 cm and a quarter tension disc infiltrometer (Fig. 1a). The infiltrometer with a quarter-disc base of 6 cm radius was positioned at the soil surface in one of the corners of the box. It allowed to impose a constant negative water pressure head at the surface. In the first series of tests the box was filled with weakly compacted sand (Hostun S31). The mean porosity of the 10 experiments was 0.495 with standard deviation of 0.015. The mean initial water content was 0.089 with standard deviation of 0.006. The applied surface pressure head was $h_{surf} = -7, -4, -2, -0.5$ and 0 cm (two tests were carried out for each value). The measured cumulative amount of infiltrating water is shown in Fig. 2a. For each value of h_{surf} we show the results of the two tests and their average.

The second series of tests was performed on sand with artificially created macropores. The macropores were made using steel pins of 2 mm in diameter, in regular spacing of 1.5 cm (Fig.

1b), resulting in the relative volumetric fractions $w_1 = 0.991$ and $w_2 = 0.009$ for the sand matrix and macropores, respectively. The porosity of the sand (not counting macropores) and the initial water content were the same as in the first series. Two experiments were performed with $h_{surf} = -2$ and -0.5 cm, and one experiment was performed for $h_{surf} = 0$. The measured cumulative infiltration curves are shown in Fig. 2b. Note that a significant acceleration of the infiltration rate is observed for $h_{surf} = 0$.

3 Governing equations

3.1 Homogeneous sand

We assume that the infiltration in homogeneous sand can be treated as an axi-symmetric process, described by the Richards equation in the following form:

$$\frac{\partial \theta_1(h)}{\partial t} - \frac{\partial}{\partial r} \left(K_1(h) \frac{\partial h}{\partial r} \right) - \frac{K_1(h)}{r} \frac{\partial h}{\partial r} - \frac{\partial}{\partial z} \left(K_1(h) \frac{\partial h}{\partial z} - K_1(h) \right) = 0 \quad (1)$$

where t – time, r – radial coordinate, z – vertical coordinate, θ_1 – volumetric water content, h – water pressure head and K_1 – hydraulic conductivity.

3.2 Sand with macropores

When the macropores are active, they form the primary conductive system. The water pressure equilibrates much faster in the macropores than in the sand matrix and thus radial local-scale water transfer between the two systems is observed (Fig. 1c). In order to capture these non-equilibrium effects we used the following generalized model for flow in double-porosity media (Szymkiewicz & Lewandowska 2006):

$$w_1 \frac{\partial \bar{\theta}_1}{\partial t} + w_2 \frac{\partial \theta_2(h)}{\partial t} - \frac{\partial}{\partial r} \left(K_r^{eff}(h) \frac{\partial h}{\partial r} \right) - \frac{K_r^{eff}(h)}{r} \frac{\partial h}{\partial r} - \frac{\partial}{\partial z} \left(K_z^{eff}(h) \frac{\partial h}{\partial z} - K_z^{eff}(h) \right) = 0 \quad (2)$$

where: w_1, w_2 – volumetric fractions of the sand and macropores, h – macroscopic pressure head (corresponding to the macropores), $\bar{\theta}_1$ – average water content in the sand at a given macroscopic point (r, z), θ_2 – water content in macropores, K_r^{eff}, K_z^{eff} – effective conductivity of the medium in radial and vertical direction. The local-scale flow at an arbitrary macroscopic point (r, z) is assumed to be radial (Fig. 1c) and is described by the following equation:

$$\frac{\partial \theta_1(h_1)}{\partial t} - \frac{\partial}{\partial \xi} \left(K_1(h_1) \frac{\partial h_1}{\partial \xi} \right) - \frac{K_1(h_1)}{\xi} \frac{\partial h_1}{\partial \xi} = 0 \quad (3)$$

with the boundary conditions: $h_1 = h_2$ at $\xi = \xi_1$ and $\partial h_1 / \partial \xi = 0$ at $\xi = \xi_2$, where ξ – local radial coordinate, ξ_1 – macropore radius, ξ_2 – radius of the soil mantle, h_1 – local-scale pressure head in sand. The effective conductivity depends on the conductivities of the two porous systems and their geometry. For the particular arrangement of macropores considered here the conductivity in horizontal direction can be obtained using the Hashin-Shtrikman formula (Lewandowska *et al.* 2005), while the conductivity in vertical direction is given by weighted arithmetic mean:

$$K_r^{eff}(h) = K_1(h) + \frac{2w_2 K_1(h_2)(K_2(h) - K_1(h))}{2K_1(h) + w_1(K_2(h) - K_1(h))} \quad K_z^{eff}(h) = w_1 K_1(h) + w_2 K_2(h) \quad (4a,b)$$

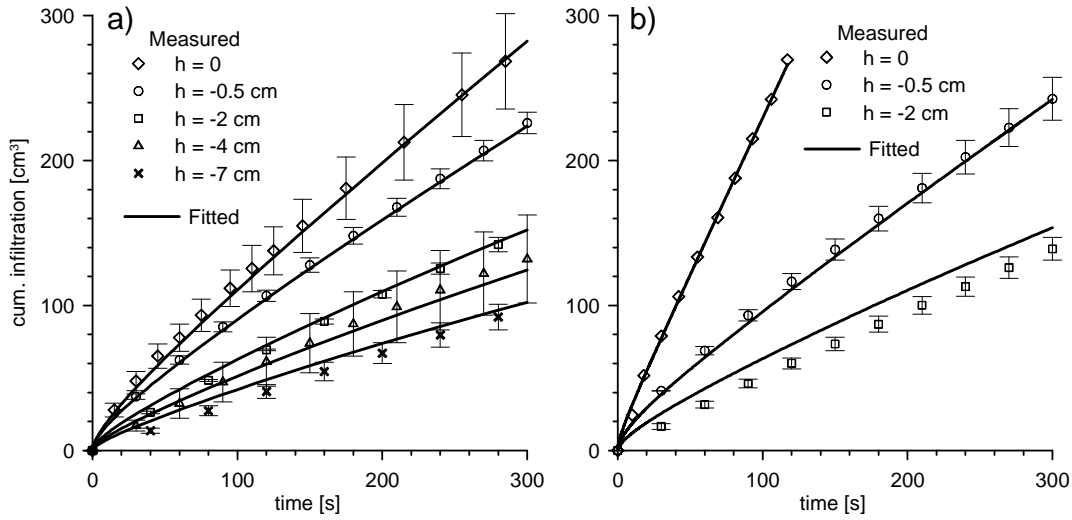


FIG. 2 – Measured and fitted cumulative infiltration curves: a) homogeneous sand, b) sand with macropores.

The model (2)-(4) remains valid also for lower values of h_{surf} , when the macropores are practically impermeable and at equilibrium with the sand matrix (Szymkiewicz & Lewandowska 2006).

Eqs. (1) and (2)-(3) were solved numerically with the DPOR-2D code developed by the authors, based on a fully implicit finite volume formulation (Szymkiewicz *et al.* 2007). The solution domain represents a quarter of cylinder with $0 \leq z \leq 18\text{cm}$ and $0 \leq r \leq 16.93\text{ cm}$, which has the same volume as the box. A constant pressure head is imposed at a part of the upper boundary ($0 \leq r \leq 6\text{ cm}$), while the other boundaries are treated as impermeable.

4 Inverse analysis

4.1 Homogeneous sand

We attempted to reproduce the experiments in homogeneous sand using a few well-known types of hydraulic functions. They are expressed in terms of the effective water saturation S_E , defined as $S_E = (\theta - \theta_R)/(\theta_S - \theta_R)$, where θ_S and θ_R denote the water content at saturation and the residual water content, respectively. The van Genuchten (1980) functions (VG) have the following form:

$$S_E(h) = \left(1 + (h/h_g)^n\right)^{-m} \quad K(h) = K_S S_E^a \left(1 - (1 - S_E^{1/m})^m\right)^b \quad (5a,b)$$

where h_g , n – soil-dependent parameters and K_S – the conductivity at saturation. If Mualem's (1976) (M) conductivity model is applied, $m = 1 - 1/n$, $a = 0.5$ and $b = 2$, while for Burdine's (1953) (B) model $m = 1 - 2/n$, $a = 2$ and $b = 1$. The Brooks & Corey (1964) functions (BC) are:

$$S_E(h) = (h_a/h)^\lambda \quad K(h) = K_S S_E^\eta \quad (6a,b)$$

where h_a – the air entry pressure, λ , η – dimensionless exponents. Eqs (6a,b) are valid for $h < h_a$, while for $h \geq h_a$ $S_E = 1$ and $K = K_S$. The exponent η is defined as $\eta = 2.5/\lambda$ for the Mualem's model and $\eta = 3/\lambda$ for the Burdine's model. It is also possible to treat η as an independent parameter and use the function (6b) with any type of the $S_E(h)$ relation (5a or 6a).

Seven sets of hydraulic functions were examined. Four of them represent the standard models: VG-M, VG-B, BC-M, BC-B. The other three sets include the conductivity function

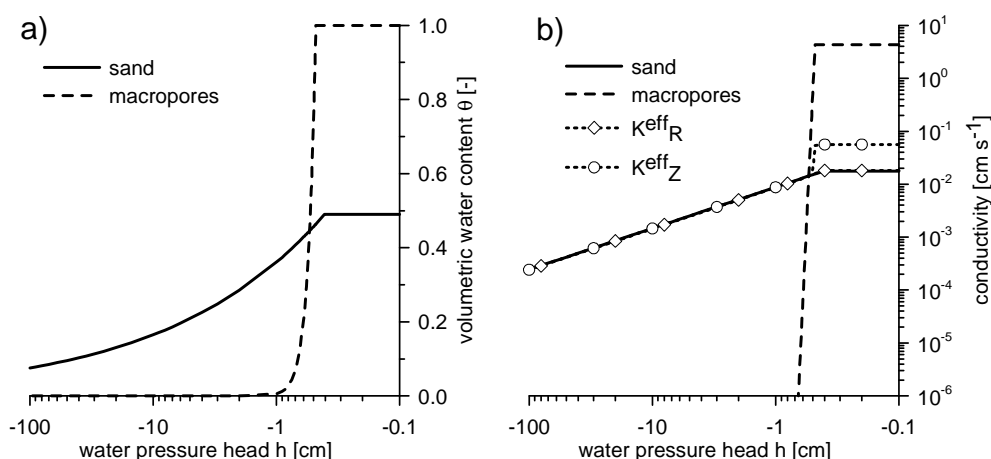


FIG. 3 – Retention (a) and conductivity (b) functions fitted for sand and macropores and the effective conductivity functions.

given by Eq. (6a) with independent parameter η combined with various retention functions: (5a) with $m = 1-1/n$ (VG1- η), (5a) with $m = 1-2/n$ (VG2- η) and (6a) (BC- η). In order to solve the inverse problem we defined the objective function as the sum of squared errors (SSQ) between the observed and predicted cumulative infiltration. The search for the parameter set which minimizes the objective function was carried out using the Marquardt-Levenberg algorithm (Press *et al.* 1992). In order to reduce the number of fitted parameters we assumed that $\theta_R = 0$ and $\theta_S = 0.495$ (i.e equal to the porosity).

TABLE 1 – Parameters fitted for homogeneous sand using various hydraulic functions

| Functions | K_S [cm s ⁻¹] | $h_g(h_a)$ [cm] | n (λ) [-] | η [-] | SSQ [cm ⁶] |
|-------------|-----------------------------|-----------------|-----------------------|------------|------------------------|
| VG-M | 1.88×10^{-2} | -18.18 | 1.34 | - | 1.47×10^4 |
| VG-B | 1.96×10^{-2} | -11.05 | 2.18 | - | 1.86×10^4 |
| BC-M | 1.24×10^{-2} | -0.37 | 0.14 | - | 1.37×10^6 |
| BC-B | 1.66×10^{-2} | -0.38 | 0.14 | - | 1.41×10^6 |
| VG1- η | 2.04×10^{-2} | -0.67 | 1.32 | 3.08 | 2.63×10^3 |
| VG2- η | 1.88×10^{-2} | -0.49 | 2.32 | 2.82 | 2.08×10^3 |
| BC- η | 1.78×10^{-2} | -0.41 | 0.34 | 2.29 | 1.90×10^3 |

Table 1 lists the fitted values of the parameters and the resulting value of the SSQ. The best results were obtained when η was fitted independently. The VG-M and VG-B models produced reasonable fits, but their SSQ was about an order of magnitude larger. Using BC-M and BC-B models we were unable to find a reasonable fit. The BC- η functions (Fig. 3a,b) gave the smallest SSQ, producing cumulative infiltration curves very close to the measured ones (Fig. 2a).

4.2 Sand with macropores

The double-porosity model requires the knowledge of hydraulic functions both for sand matrix and for the macropore system. For the sand matrix we used the previously identified BC- η functions. For the macropores we assumed step-like retention and conductivity functions. This was achieved using BC- η model with $\lambda = 7$ and $\eta = 7$, forcing $S_E(h)$ and $K(h)$ to tend to zero rapidly for $h < h_a$. We also assumed that $\theta_R = 0$ and $\theta_S = 1$. The theoretical values of the air-

entry pressure and the conductivity at saturation can be calculated from the Laplace law and the Poiseuille law, i.e $h_a = -0.149/\xi_1 = -1.5$ cm and $K_{s,2} = \rho g(\xi_1)^2/(8\mu) = 122.6$ cm s⁻¹, respectively, where ξ_1 – the macropore radius, ρ – water density, g – gravitational acceleration and μ – water dynamic viscosity. However, using these values resulted in a very large overestimation of the infiltration rate. Thus we decided to identify h_a and K_s using an inverse approach, while keeping the other parameters constant. The values obtained by numerical optimization are $h_a = -0.48$ cm and $K_s = 4.34$ cm s⁻¹, with SSQ = 9.71×10^4 cm⁶. In Figs 3a,b we present the fitted retention and conductivity functions of the macropores, as well as the effective conductivity of the double-porosity medium in horizontal and vertical direction, calculated from Eqs (4a,b). Note that the presence of the macropores practically do not alter the medium conductivity in horizontal direction, while significantly increasing the vertical conductivity close to saturation. In Fig. 2b the fitted cumulative infiltration curves for sand with macropores are compared with the experimental results.

5 Conclusions

The hydraulic functions required by the double-porosity model were successfully identified using numerical inverse analysis. In particular the increased infiltration rate for $h_{surf} = 0$ is well represented using the fitted parameters. The discrepancy between the theoretical and fitted values of h_a and K_s for macropores can be attributed to partial clogging of the macropores with sand, which reduces their diameter and increases the irregularity of the lateral surface.

Acknowledgments

This research was performed in the framework of the ECCO/PNRH Program “Transferts complexes en milieu poreux et ressources en eau” (INSU-CNRS).

References

- Brooks, R. & Corey, A. 1964 Hydraulic properties of porous media. Hydrology Paper No. 3, Colorado State University, Fort Collins.
- Burdine, N. 1953 Relative permeability calculations from pore size distribution data. *Petrol. Trans. Am. Inst. Min. Eng.* **198**, 71-77.
- Lewandowska, J., Szymkiewicz, A., Burzyński, K. & Vauclin, M. 2004 Modeling of unsaturated water flow in double porosity soils by the homogenization approach. *Adv. Water Resour.* **27**, 283-296.
- Lewandowska, J., Szymkiewicz, A. & Boutin, C. 2005 Modeling of unsaturated hydraulic conductivity of double porosity soils. In Actes de 17^{ème} Congrès Français de Mécanique, Troyes, Sept. 2005.
- Lutz, P. 1998 Influence des macropores sur l'infiltration d'eau dans les sols non saturés : caractérisation hydrodynamique par infiltrométrie sous pression contrôlée. Mémoire de DEA, Université Joseph Fourier, Laboratoire d'étude des Transferts en Hydrologie et Environnement, 46 pp.
- Mualem, Y. 1976 A new model for predicting the hydraulic conductivity of unsaturated porous media. *Water Resour. Res.* **12**, 513-522.
- Press, W.H., Flannery, B.P., Teukolsky, S.A., & Vetterling, W.T. 1992 Numerical recipes in Fortran. Cambridge University Press.
- Richards, L.A. 1931 Capillary conduction of liquids through porous medium. *Physics* **1**, 318-333.
- Szymkiewicz A., & Lewandowska, J. 2006 Unified macroscopic model for unsaturated water flow in soils of bimodal porosity. *Hydrological Sciences Journal* **51**, 1106-1124.
- Szymkiewicz A., Lewandowska, J., Angulo-Jaramillo, R. & Butlańska J. 2007 Two-scale modeling of unsaturated water flow in the double-porosity medium under axi-symmetrical conditions, submitted.
- van Genuchten, M. Th. 1980 A closed form equation for predicting the hydraulic conductivity of unsaturated soils. *Soil Sci. Soc. Am. J.* **44**, 892-898.